Further investigation into regime transition from bubbling to turbulent fluidization

Haiyan Zhu and Jesse Zhu
Departments of Chemical and Biochemical Engineering,
University of Western Ontario, London, Ontario, N6A 5B9

Introduction

Over the last fifty years gas-solids fluidized beds have played a very important role in many areas in the process industry, especially in chemical and petroleum industries. The existence of different flow regimes in fluidized beds at different operating conditions has been known for a long time and numerous studies have been carried out to define the flow regimes [1-6]. It is well accepted that with increasing gas velocity, the bed goes through particulate fluidization, bubbling fluidization, turbulent fluidization, fast fluidization and pneumatic transport [7]. According to the experimental evidence available in the literature so far, a common way to classify the flow regimes is to determine the transition velocities by means of different measurement techniques and interpretation methods [6, 8-9]. The transition velocities have been found to be influenced by many factors such as solids properties [10-12], solids inventory [13], column diameter [14], distributor design [15-16], operating temperature and pressure [17-18], the measuring techniques and data analysis methods [19]. Therefore it should be very careful to compare the regimes transition velocities obtained with different flow systems and different data analysis methods.

Although lots of fluidized beds are operated in turbulent flow regime where minimizing entrainment and maximizing gas throughput are needed, e.g., FCC regeneration, silicon chloridization and particle drying, the hydrodynamic properties of this special flow regime are still not well understood, and the regime transition from bubbling to turbulent fluidization are not completely clear. One of the earliest works on quantitatively studying the turbulent fluidization was performed by Lanneau (1960) [20] using a capacitance probe. The local bed densities were measured, and with increasing gas velocity, there was a sudden drop in the average bed density, accompanied with a decrease in amplitude and increase in frequency of fluctuation a local voidage. In 1971, Kehoe and Davidson [21] extended their work in a slugging to higher velocity fluidized beds with capacitance probe, X-ray and cine photography, and first introduced the turbulent fluidization regime into the flow regime diagram. Yerushalmi et al. [22] first clearly proposed and measured the transition criterion to identify the transition from bubbling/slugging to turbulent fluidization. They defined two gas velocities to demark the transition: U_c (at which the standard deviation of pressure fluctuations reached a maximum) demarcating the beginning of the transition to turbulent fluidization, and U_k (at which the standard deviation of the pressure fluctuations levels off) indicating the end of the transition and the onset of turbulent fluidization. Since early work of Yerushalmi, extensive studies have been carried out to quantify the two transition velocities and also raised controversies in the literature on the definition of the transition. Some researchers found that there was no existence of U_k according to their

experimental results and even question the existence of turbulent fluidization as a distinct flow regime [23-25]. Rhodes and Geldart [24] even pointed out that the transition characterized by U_k is actually a transfer of solids from the fluid bed to the freeboard instead of a fundamental change in the flow structures in the bed. Some other researchers suggested that the turbulent regime starts at U_c [10, 26-27].

Numerous studies have been carried out to define the flow transition from bubbling to turbulent fluidization and interpreted what was occurring during this regime transition, however few of them have ever investigated this subject from a localized point of view. The objectives of this work are: 1) to further investigate the transition from bubbling to turbulent fluidization based the measurements of transient solids concentrations (local) and differential pressure drops (global); 2) to compare the global and local regime transition phenomena and velocities; 3) to study the effects of static bed height and interval distance between pressure measurement ports on the regime transition velocities.

Experiments setup

Experiments were carried out in a gas-solid fluidized bed (0.267m i.d. × 2.5m high) at ambient temperature and pressure, as shown in Fig.1. The solid material was spent fluid catalytic cracking (FCC) catalyst with a particle density of 1800 kg/m^3 and a Sauter mean diameter of 62 μm. The turbulent fluidized bed mainly consists of three parts: 1) a Plexiglas column (with an i.d. of 267 mm and a height between distributor and top of 2.464 m) where particles are fluidized upwards; 2) a disengaging section at the top of the fluidizing column with a diameter of 667 mm and a total height of 1.745 m; 3) a recycle loop including three cyclones in series and a bag filter to capture the entrained particles and return them to the bottom of the column, and a small fluidized bed in the loop, fluidized at a superficial velocity just above U_{mf}, to prevent possible plugging in the return pipes. To minimize the buildup electrostatic effects, the whole system was electrically grounded. Air was fed to the bed through a porous material distributor and its flow rate was measured by an orifice plate connected to a water manometer.

Pressure ports are installed vertically along the column wall, connecting to the differential pressure transducers, which are interfaced with a personal computer via a 16-bits A/D converter for real-time data acquisition. The transducer output signals are linearly proportional to the pressure drop in the range of 0 to 10 kPa. The pressure ports are installed at five bed heights, 0.3, 0.5, 0.7, 0.9, 1.3 m above the gas distributor, which are above the primary bubble formation and coalescence controlled region [13]. The fluctuations of the differential pressure signals were measured over distances of 0.2, 0.2, 0.2, and 0.4 m. The signals of the differential pressure fluctuations are sampled with a frequency of 1000 Hz and stored temporally on disks. The total acquisition time is 30s and thus the maximum length of the time series is 30,000 points.

Reflective-type optical fiber probes are effective tools for measuring the local voidage in fluidized beds [15, 29-32]. Their small size does not considerably disturb the overall flow structure. More importantly, they are nearly free of interference by temperature, humidity, electrostatics and electromagnetic fields [33].
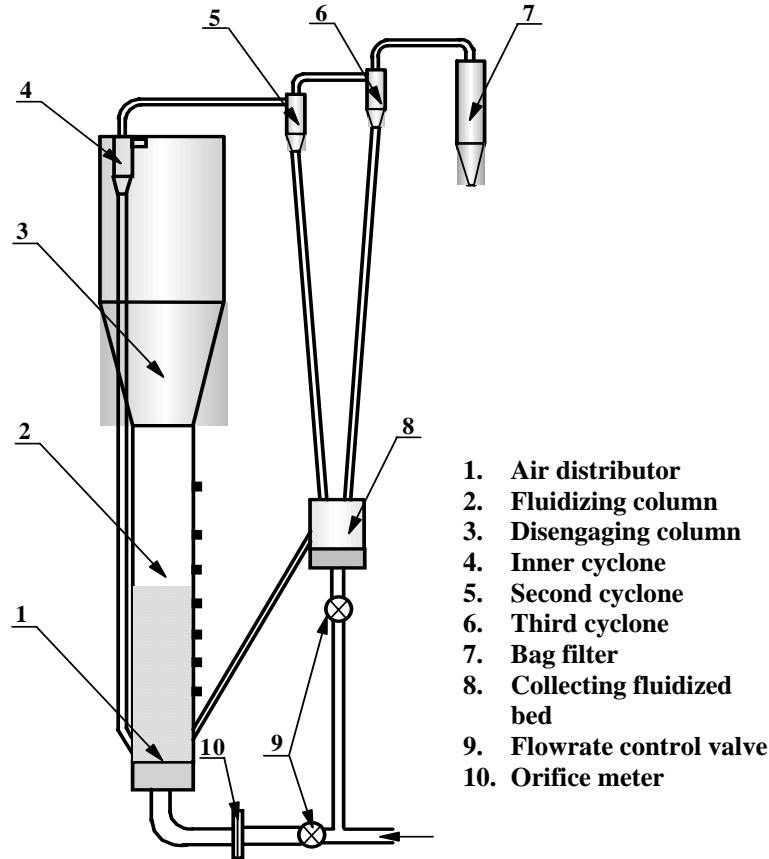
Fig.1.   Schematic drawing of the turbulent fluidized bed

1. **Air distributor**
2. **Fluidizing column**
3. **Disengaging column**
4. **Inner cyclone**
5. **Second cyclone**
6. **Third cyclone**
7. **Bag filter**
8. **Collecting fluidized bed**
9. **Flowrate control valve**
10. **Orifice meter**

The optical fiber probes used for our experiments as shown in Fig.2 are model PV-5, produced by the Institute of Process Engineering, Chinese Academy of Sciences, which can measure solids concentration at four different positions simultaneously. The diameter of the probes is 4 mm, consisting of both light emitting and receiving quartz fibers, arranged in an alternating array, corresponding to emitting and receiving layers of fibers. The diameter of the fibers is 25 um. In order to prevent particles from occupying the blind zone, a glass cover was placed over the probe tip. The received light reflected by the particles is multiplied by the photo-multiplier and converted into voltage signals. The voltage signals are further amplified and fed into a PC. Because the relationship between the output signals of the optical fiber probe and the solids concentrations is nonlinear, a reliable calibration is required to ensure that the output correctly represents the measurement. The calibration was carried out in a stable gas-solid downer system with a small enough diameter (1/2 inch) so that a local measurement could yield a cross-sectionally averaged value. Details of the calibration system have been described by Zhang et al. [33]. The solids volume concentration values range from 0 to 0.56 which corresponding to the solids concentration in a loosely packed bed.

In order to obtain more accurate representation of radial solids concentration profiles, three measurement ports are installed around the periphery of the column to measure the solids concentration. To ensure the validity and repeatability of sampled signals, for

each run the sampling time is 30s with a frequency of 1 kHz, and at least three samples are taken at each measuring position.
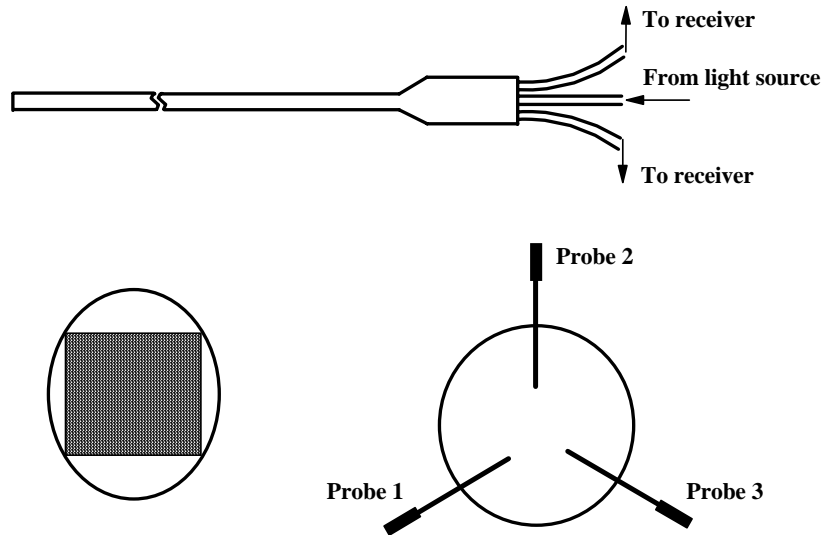
Fig. 2 Schematic of the solids concentration-velocity fiber optic probe

Regime transition velocities based on the measurements of pressure fluctuations

Pressure fluctuations are one of the most commonly measured parameters to study the global hydrodynamic behaviors of fluidized beds, and can be used to determine the regime transition velocities, and to validate hydrodynamic models of fluidized beds [8, 34-36]. Differential pressure measurements filter out the signals arising from pressure waves originating outside the measurement volume and provide more information about the localized measuring volume [37].

The axial differential pressure profiles along the column are displayed in Fig.3 (a) for various superficial gas velocities (U_g = 0.02 ~ 1.4 m/s). The corresponding standard deviations of pressure fluctuations, σ, are given in Fig.3 (b). During the experiments, the static bed height was kept at 0.9 m (around 3 times of the column diameter). The superficial gas velocities shown in this figure correspond to operating conditions from bubbling fluidization to turbulent fluidization.

It can be seen in Fig.3 (a) that with increasing U_g, the pressure gradient profiles at all three heights initially decrease quickly and then reach a stable value, with further increasing superficial gas velocity, it decreases again, but in a much slower rate. Fig.3 (a) also shows that at the same U_g, the differential pressure values decrease with increasing bed height. This may be attributed to the bubble growth, which growing with the height, and the large mount of particle entrainment near the top of the dense bed. And for the lower axial positions, there is a delay for the first decrease point: e.g., for H = 0.6 m, the pressure begins to decrease after the U_g reaches 0.3 m/s; and for H = 0.4m, U_g rises to 0.5 m/s.

(a)

(b)
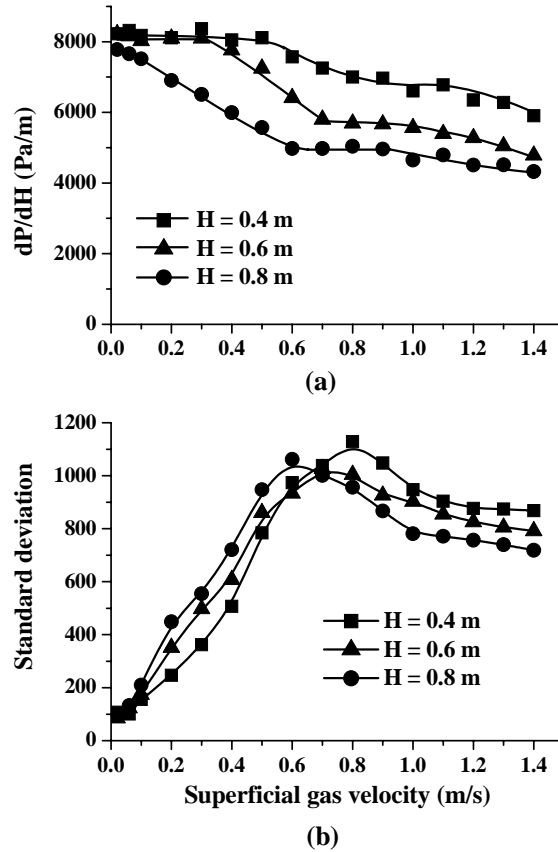
Fig. 3. Determination of the transition velocity by analysis of the standard deviation of differential pressure fluctuations

Fig. 3(b) shows that for all axial positions, the standard deviation, σ, reaches its peak with increasing U_g around 0.6-0.8 m/s and then decreases with further increasing gas velocity. And, the standard deviation does not level off until U_g is beyond 1.2 m/s. According to the definition introduced by Yerushalmi and Cankurt [23], the gas velocity at which σ reaches its maximum is referred to as the transition velocity U_c from bubbling to turbulent regime. It is interesting to note that σ at upper levels is higher than that at lower position until gas velocity reaches U_c, after that point, the highest value for σ always appears at lowest positions. Another important observation is that with increasing bed height the transition velocity U_c shrifts to lower value. It can be contributed to the fact that the generation of the bubbles mainly happens just above the gas distributor [36], and the bubbles grow with the bed height. With increasing U_g, the bubbles reach their maximum size at the upper section of the fluidized bed first, then the flow regime at this section transits into turbulent fluidization first. These results imply that under lower gas velocities the main pressure fluctuations are generated by the passage and burst of bubbles. As a result, the pressure fluctuations become less than the lower sections, under lower gas velocity.

Effects of static bed height H_o on flow regime transition

The differential pressure fluctuations obtained at two different static bed heights (H_o = 0.9 m and 1.2 m) as a function of superficial gas velocity at different axial positions are compared in Fig.4.

(a) H_0 = 0.9 m

(b) H_0 = 1.2 m
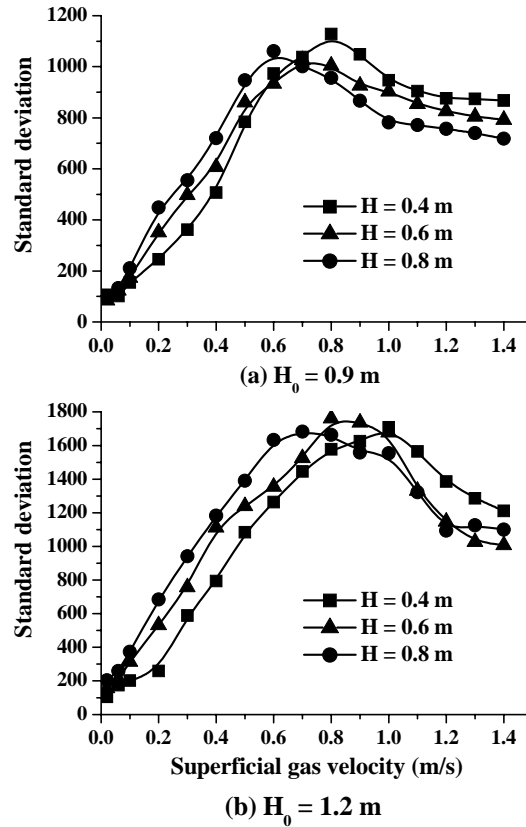
Fig. 4 Effects of static bed height H_0 on pressure fluctuations

Significant variations in σ are clearly seen in this figure. With increasing the static bed height, H_o, from 0.9 m to 1.2 m, the standard deviations, σ, at all operating conditions and at all measuring positions are increased, indicating that with increasing H_o the hydrodynamic behaviors in the fluidized bed become more complex. Furthermore, it was also found that with increasing H_o the flow regime evolves more gradually from bubbling to turbulent fluidization. Instead of a step change when H_o is at 0.9 m, the rate of increase and decrease of σ in all positions becomes very slow around the transition point U_c when H_o is raised to 1.2 m.

The transition velocities U_c obtained with the two different H_o at different bed heights are plotted in Fig.5. It shows more clearly that with increasing H_o, U_c shifts to higher velocity at the same axial level, but the differences become smaller with increasing axial level, it implies that the effects of increasing H_o on regime transition is larger in lower section of the bed. At the same time, it is also worth noting that the transition velocity U_c appears to remain the same if the relative distance from the measuring point to the initial static bed height is similar. For example, comparing the case when H_o is 0.9 m and the measurement point is at H = 0.6 m, with the case when H_o is 1.2 m and with the

measurement point at $H = 0.8$ m, the transition velocity, U_c, is about 0.7 m/s for both cases. This result is reasonable; because the regime transition from bubbling to turbulent fluidization corresponds with the rapid solids entrainment and bubbles' burst, which happen first at the upper bed surface, then transfer downwards with increasing U_g. This means that the relative distance from the investigated position to upper bed surface has greater influence on the corresponding transition velocity, U_c, than the absolute distance above gas distributor.
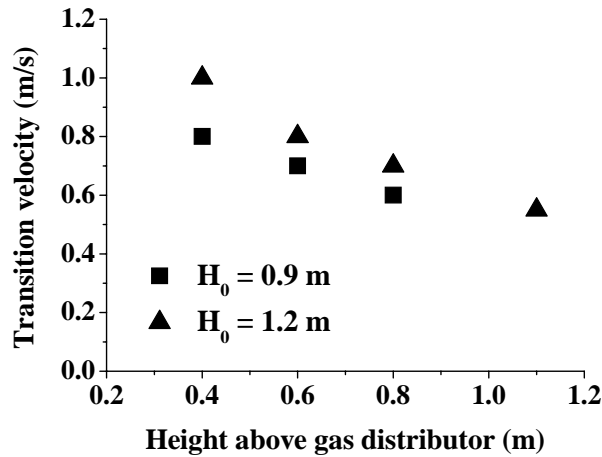
Fig. 5 Effects of static bed height H_0 on regime transition velocity

Effects of distance between pressure tubes on flow regime transition

The effects of distance between differential pressure tubes on flow regime transition were examined with two spacings, 0.2 m (from $Z = 0.5$ to 0.7 m) and 0.6 m (from $Z = 0.3$ to 0.9 m), and at two different static bed heights ($H_0 = 0.9$ and 1.2 m). The measured pressure fluctuations as a function of superficial gas velocity are plotted in Fig. 6.

For the same measuring level ($\overline{H} = 0.6$ m) and initial static bed height ($H_0 = 0.9/1.2$ m), with increasing the spacing of the pressure probes, the intensity of the differential pressure fluctuations decreases and the degree of the difference increases first with superficial gas velocity and, after reaching a maximum, levels off with increasing gas velocity further. It implies that, although pressure fluctuations from other locations can be filtered out by reducing the tube spaces, more inner pressure fluctuations tend to be damped out by increasing the spacing. Therefore, caution should be exercised when choosing the pressure tube spacings. This result is in contrast with that reported by Bi and Grace [20], who claim that the intensity of pressure fluctuations is lower for the smaller spacing and the spacing between the pressure ports does not affect the transition velocity. This may be caused by the fact that for their larger spacing which is from $Z = 0.03$ to 0.41 m, the location of the lower pressure tube ($Z = 0.03$ m) was too close to the gas distributor, where larger pressure fluctuations have been generated by gas distributor effect, as observed by Chen et al. [13] and Fan et al. [39]. It is also worth noting that with increasing the spacing between the pressure tubes, there appears a long plateau in the standard deviation profiles for the larger spacing, indicating that for the larger

spacing, which represents a larger measuring volume, the regime transition from bubbling to turbulent fluidization becomes a more gradual process. From Fig. 6, we can see that with increasing static bed height from 0.9 to 1.2 m, the effect of spacing of pressure tubes on regime transition velocity becomes larger and the process of the transition also last longer.
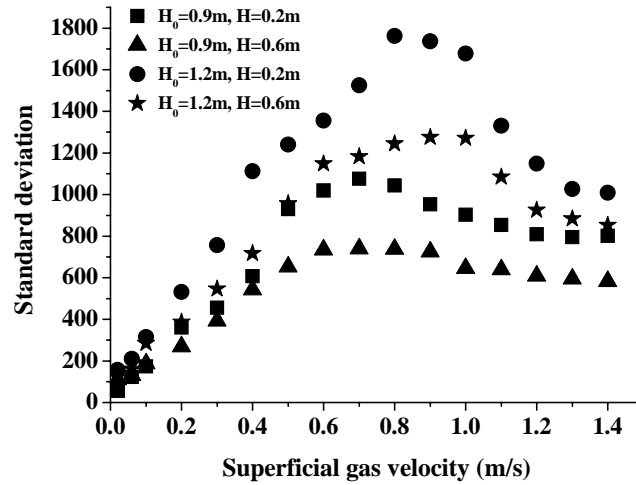
Fig. 6 Effects of spacing of pressure tubes on flow regime transition (*H* = 0.6 m)

Local regime transition

Very little attention has been given to investigating the flow regime transition with respect to local flow structures, this is hindering a better understanding of the evolution process of the flow regime transition happened in the fluidized beds. Here the local transient solids concentration were carefully measured with optical fiber probes, and the analyses on the fluctuations of the local solids concentration have revealed how local flow structure transits from bubbling to turbulent fluidization regime. Fig. 7 presents the time-averaged solids concentration (a) and its corresponding standard deviation (b) profiles as a function of gas velocity (U_g = 0.06 ~ 1.4 m/s), taken at 5 radial positions (r/R = 0, 0.5, 0.74, 0.87, 0.98). As mentioned before, the solids concentrations are measured from three different radial directions, and the final result for each radial position is calculated by averaging the measurements obtained by these three solids concentration fiber probes.

As shown in the Fig.7 (a), with increasing superficial gas velocity, U_g, significant differences among the results are observed at five radial positions. For the central region ($0 < r/R < 0.74$): the solids concentration decreases quickly with increasing U_g, reaches a relatively stable level, and then decreases again. For the wall region ($0.87 < r/R < 1$), the changes in the time-averaged solids concentration with respect to U_g are relatively slow. It is can be seen from the Fig.7 (a) that with increasing U_g from 0.02 to 1.4 m/s, the solid concentration is decreased by ~ 70% at the center ($r/R = 0$), but ~ 4% at the wall ($r/R = 0.98$).
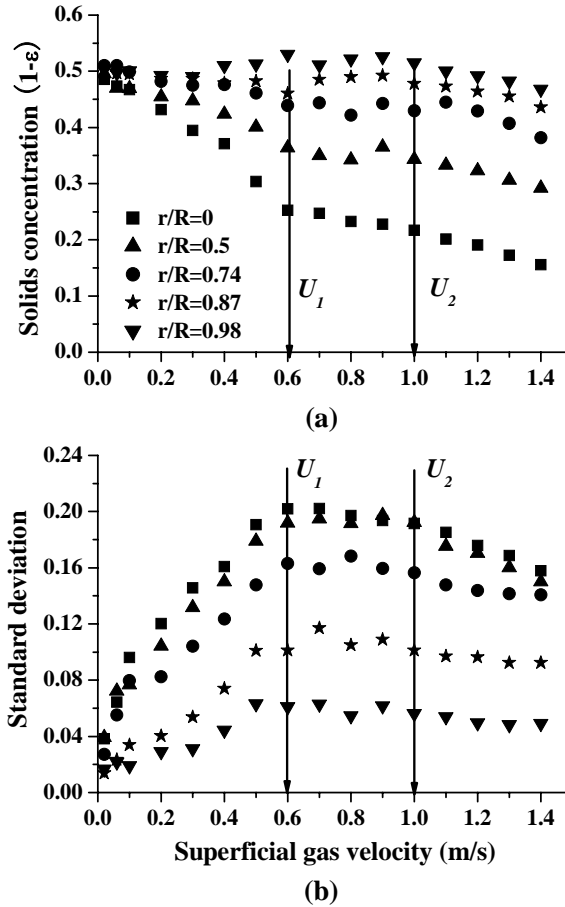
**Fig. 7 (a) Solids concentration profiles as a function
of U_g at different radial positions, (b) corresponding
standard deviation profiles (H_0 = 0.9 m, H = 0.6m)**

Fig.7 (b) shows that the magnitude of the fluctuations in the center is much higher compared to the wall region, indicating that the flow is more chaotic at the central region and relatively uniform near the wall. The standard deviation profiles also clearly present two new discoveries corresponding to an incipient turbulent fluidization velocity (U_1) and complete turbulent fluidization velocity (U_2). It can be concluded that the local flow transition happens at different times at different radial positions and cover a range of operating conditions. It is worth noting that the transition occurs quite sharply at $r/R =$ 0 and then the transition process becomes more and more gradually outwards to the wall. For the near wall region ($0.87 < r/R < 0.98$), although the variation trend of solids concentration profiles is similar to that in the central region, the corresponding fluctuations profiles are different: it remain almost constant after reach their maximum values at $U_g = 0.6$ m/s, implying that there is no further regime transition happening in this region after $U_g = 0.6$ m/s. But we have to mention that this result is just got from measured velocities within the range $0.02 < U_g < 1.4$ m/s.

In order to give a clearer picture about regime transition process for a whole cross section of fluidized bed, typical solids concentration profiles as a function of gas velocity from three different radial directions are shown in Fig.8 measured at radial

position $r/R = 0.16$ and axial level of $H = 0.6$ m above gas distributor (a), also included in this figure are plots of standard deviation distribution corresponding to the instantaneous solids concentration (b).
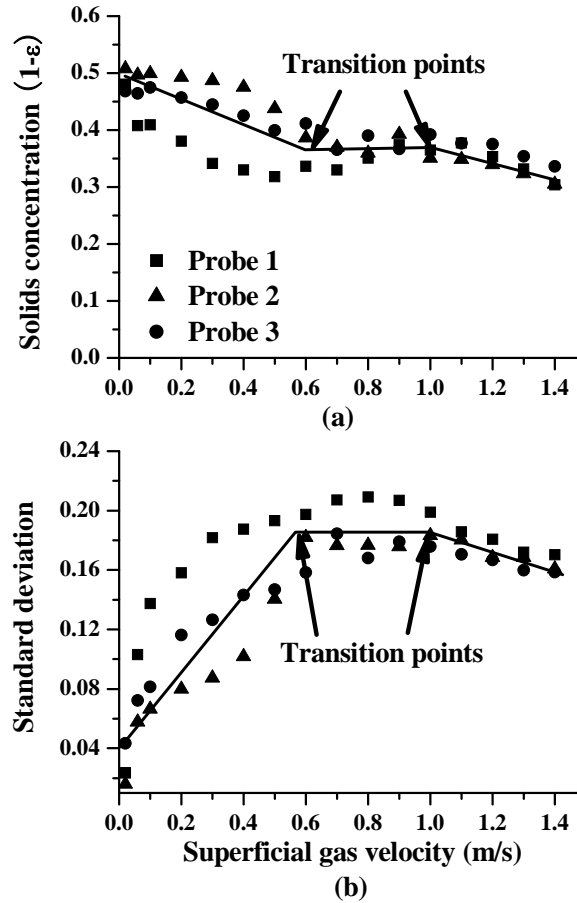
Fig. 8 (a) Solids concentration profiles as a function of U_g measured by three probes from three different radial directions, (b) corresponding standard deviation profiles (H_0 = 0.9 m, H = 0.6m, r/R = 0.59)

The results show that, under all operating conditions (gas velocities), there are always differences among the measurements obtained from three radial directions, especially under lower gas velocity ($< U_c \sim 0.7$ m/s), indicating a non-radial symmetric flow structure. The degree of the non-radial symmetry increases with the gas velocity until the velocity reaches U_c. Further increasing the gas velocity, the non-radial symmetric flow structure becomes not obvious, although there still exist small differences. Similar flow structures are reported by Du et al. [40] measured with Electrical Capacitance Tomography (ECT) techniques. However, the developing trends along the three radial directions with gas velocity are similar. With increasing U_g, solids concentration at all radial positions decreases, and three evolution stages can be identified. First, there is a quick decrease in the solids concentration, and reaches a stable value at velocity value around 0.7 m/s until the gas velocity reaches 1.0 m/s, then it continue decreasing again. The similar transition points are also found at the standard deviation profiles.

Comparison between the local and global flow regime transition velocities

As discussed before, pressure fluctuations can be used to characterize global transition, while the fiber optic probes give more local information. Fig.9 shows the comparison between the transition velocities obtained from standard deviation analysis of local solid concentration measured at the axial level $H = 0.6$ m ($H_0 = 0.9$ m), but at 11 different radial positions and that obtained from differential pressure fluctuation analysis at the same section (from $H = 0.5$ to 0.7 m).

In Fig. 9, the difference in the transition velocities defined by the two methods is clearly revealed. It is shown that at each radial position the local flow regime transition from bubbling to turbulent fluidization is a gradual process that lasts over a range of gas velocity. The local transition velocity strongly depends on the radial position, with moving outwards towards the wall, we find an increase in the transition velocity. For example, it ranges from 0.6 to 0.7 m/s at $r/R = 0$, and 0.7 to 1.2 at $r/R = 0.87$, suggesting that the transition takes place first at the center region and develops outwards towards the wall. Furthermore, when closing to the wall, there only exists the first transition velocity. This result is in agree with the findings of previous studies on local voidage fluctuations measured by electrical capacitance tomography system [41]. This local transition process is different than the global process, which is based on the measurements of differential pressure fluctuations. As shown in Figure 3(b), the transition velocity is around 0.7 m/s for this whole cross-section ($\overline{H} = 0.6$ m), and this transition happens relatively abrupt instead of a gradual process.
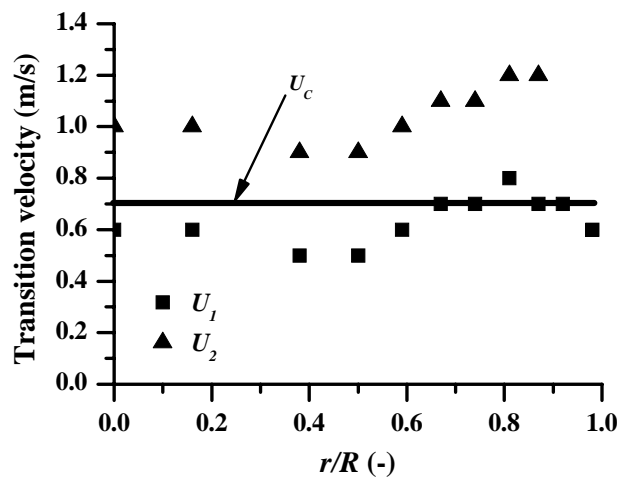
Fig. 9. Comparison of transition velocity from fluctuations analysis of local solids concentration and differential pressure ($H = 0.6$ m; $H_0 = 0.9$ m)

It can be noted that the transition velocity, U_c, determined from the differential pressure fluctuations is always higher than U_1 and lower than U_2 at almost all radial positions and the local flow regime transition velocities are strong functions of radial position. When comparing the regime transition identified by local solids concentration and differential

pressure, we can conclude that the standard deviation obtained with the differential pressure fluctuations represent the overall hydrodynamic behaviour, while the direct solid concentration measurements provide more hydrodynamic information about the localized measuring point. These results indicate that there exists an intermediate transition between the bubbling and turbulent fluidization marked with two transition velocities when we localized our investigating volume.

Conclusions

For better understanding of the flow behaviors and for fundamental modeling of the multiphase fluidization systems, it is of prime importance to have a complete and reliable knowledge of the regime transition taking place in these systems. In this paper, extensive experiments are performed to investigate the transition from bubbling to turbulent fluidization in the fluidized bed using differential pressure transducers and optical fiber probes. It presents detailed local and global flow regime transition process, and special efforts are made to extend the knowledge of the transition velocity, U_c, based on the standard deviation analysis of local solid concentration and differential pressure measurements.

The transition velocity, U_c, determined from differential pressure fluctuations, was found to increasing with decreasing axial locations, suggesting that regime transition from bubbling to turbulent fluidization occurs first at upper region of the fluidized bed and develops downward. The effect of initial static bed height H_0 on U_c is also reported, with increasing H_0 from 0.9 to 1.2 m, U_c increased from 0.6 to 0.7 m/s at $H = 0.8$ m and from 0.8 to 1.0 m/s at $H = 0.4$ m. The results also show that the relative distance from the investigated position to upper bed surface has greater influence on the corresponding transition velocity, U_c, than the absolute distance above gas distributor. For the same H_0, increasing the spacing between two pressure tubes let to lower pressure fluctuations and the appearance of two transition velocities.

The local flow regime transition was studied with standard deviation analysis of local solids concentrations, measured at 11 different radial positions from three radial directions. Two transition points are clearly found and they shift to higher velocity with moving outward towards wall region. Furthermore, the range between these two point also increases with moving outwards, and in near wall region ($r/R = 0.92 \sim 0.98$), the second transition point is no longer found.

The experimental results suggest that marking the regime transition from bubbling to turbulent fluidization with just one transition velocity is not adequate. Our analysis reveals that the transition velocity strongly depends on both axial and radial positions, and it is important to study the flow system in details to properly characterize how the regime transition occurs. The standard deviation analysis of local solid concentration measured provides a good understanding of the local regime transition. Comparison of the transition velocity results determined by local solid concentration fluctuations (U_1 and U_2) and differential pressure fluctuations (U_c) reveals that U_c is always higher than U_1 and lower than U_2 at all radial positions, indicating that the differential pressure

measurements represent averaged flow behaviour of the measuring section between two pressure tubes.

The measurements present a non-radial symmetric flow structure. The degree of the non-radial symmetry increases with the gas velocity until the velocity reaches U_c. Further increasing the gas velocity, the non-radial symmetric flow structure becomes not obvious, although there still exist small differences among the three measurements.

Notation

dP	=	pressure drop, Pa
H	=	bed height, m
H_o	=	initial static bed height, m
$\overline{H}$	=	average bed height, m
r	=	radial distance from column axis, m
R	=	radius of column, m
U_1	=	transition velocity at which standard deviation of local solids concentration reaches a maximum, m/s
U_2	=	transition velocity at which standard deviation of local solids concentration begin to decrease, m/s
U_c	=	transition velocity at which standard deviation of pressure fluctuations reaches a maximum, m/s
U_g	=	superficial velocity of gas in bed, m/s
U_k	=	superficial gas velocity corresponding to leveling out of pressure fluctuation amplitude as U_g is increased, m/s
U_{mf}	=	superficial gas velocity at minimum fluidization, m/s
ε	=	voidage
σ	=	standard deviation

Reference

1. Zenz, F.A. Two-phase fluidized-solid flow, Industrial and Engineering Chemistry. 1949; 41: 2801-2806.
2. Yerushalmi, J., Cankurt, N. T., Geldart, D. and Liss, B. Flow Regimes in Vertical Gas-Solid Contact Systems. AIChE Symp. Ser. 1978; 74(176):1-12.
3. Grace, J.R. Contacting modes and behaviour classification of gas-solid and other two-phase suspension. Canadian Journal of Chemical Engineering. 1986; 64:353-363.
4. Hirama, T., Takeuchi, T., Chiba, T. Regime classification of macroscopic gas-solid flow in a circulating fluidized-bed riser. Powder Technology. 1992; 70: 215-222.
5. Bi, H.T., Grace, J.R. Flow regime diagrams for gas solid fluidization and upward transport, Int. J. Multiphase flow, 1995; 21:1229-1236.
6. Smolders, K., Baeyens, J. Gas fluidized beds operating at high velocities: a critical review of occurring regimes. Powder Technology. 2001; 119:269-291.
7. Lim, K.S., Zhu, J.X., Grace, J.R. Hydrodynamics of gas-solid fluidization. Int. J. Multiphase flow. 1995; 21:141-193.
8. Bai, D., Shibuya, E., Nakagawa, N, Kato, K. Characterization of gas fluidization regimes using pressure fluctuation. Powder Technology. 1996; 87:105-111.
9. Bai, D., Issangya, A.S., Grace, J.R. Characteristics of gas-fluidized beds in different flow regimes, Ind. Eng. Chem. Res., 1999; 38:803-811.
10. Cai, P., Jin, Y., Yu, Z.Q., Wang, Z.W. Mechanism of flow regime transition from bubbling to turbulent fluidization. AIChE. Journal. 1990; 36: 955-956.
11. Grace, J. R., Sun, G. Influence of particle size distribution on the performance of fluidized bed reactors. Canadian Journal of Chemical Engineering. 1991; 69:1126-1134.
12. Gauthier, D., Zerguerras, S., Flamant, G. Influence of the particle size distribution of powders on the velocities of minimum and complete fluidization. Chemical Engineering Journal. 1999; 74:181-196.
13. Chen, Sha-Peng, Yu, Zhi-Qing, Jin, Yong, Cai, Ping. Investigation on the vertical division of flow regions in a gas-solid fluidized bed by means of coherence function. Powder Technology. 1993; 75(2):127-131.
14. Kim, SungWon, Kirbas, Gorkem, Bi, Hsiaotao, Lim, C. Jim, Grace, John R. Flow behavior and regime transition in a high-density circulating fluidized bed riser. Chemical Engineering Science. 2004; 59:3955-3963.
15. Ellis, N., Bi, H.T., Lim, C.J., Grace, J.R. Hydrodynamics of turbulent fluidized beds of different diameters. Powder Technology. 2004; 141:124-136.
16. Svensson, A., Johnsson, F., Leckner, B. Fluidization regimes in non-slugging fluidized beds: The influence of pressure drop across the air distributor. Powder Technology. 1996; 86:299-3123.
17. Sathiyamoorthy, D., Horio, Masayuki. On the influence of aspect ratio and distributor in gas fluidized beds. Chemical Engineering Journal. 2003; 93:151-161.
18. Choi, J. H., Ryu, H. J., Shun, D. W., Son, J. E., Kim, S. D. Temperature effect on the particle entrainment rate in a gas fluidized bed. Industrial and Engineering Chemistry Research. 1998; 37:1130-1135.

19. Cui, Heping, Chaouki, Jamal. Effects of temperature on local two-phase flow structure in bubbling and turbulent fluidized beds of FCC particles. Chemical Engineering Science. 2004; 59:3413-3422.

20. Bi, H.T., Grace, J.R. Effect of measurement method on the velocities used to demarcate the onset of turbulent fluidization. Chemical Engineering Journal. 1995; 57:261-271.

21. Lanneau, K. P. Gas-solids contacting in fluidized beds. Transactions of the Institution of Chemical Engineers. 1960; 38:125-137.

22. Kehoe, P.W.K., Davidson, J.F. Continuously slugging fluidized beds. Chemeca '70, Institution of Chemical Engineers Symposium Series. Australia: Butterworths. 1970; 33:97-116.

23. Yerushalmi, J. and Cankurt, N. T. Further Studies of the Regimes of Fluidization. Powder Technology. 1979; 24:187-205.

24. Rhodes, M. J., Geldart, D. Transition to turbulence? In K. Østergaard, A. Sørensen, Fluidization V. New York: Engineering Foundation. 1986:281-288.

25. Perales, F., Nicolai, R., Coll, T., Llop, M.F., Puigjaner, L., Arnaldos, J., Casal, J. In Casal, J., Arnaldos, J. Fluidization and Fluid/Particle Systems. Universitat Politecnica de Catalunya, Girona, Spain. 1990:111-118.

26. Rhodes, M. J. What is turbulent fluidization? Powder Technology. 1996; 88:3-14.

27. Sun, G. L., Chen, G. Transition to turbulent fluidization and its prediction. In Grace, J.R., Shemilt, L.W., Bergougnou, M.A. Fluidization VI. New York: Engineering Foundation. 1989:33-40.

28. Gonzalez, A., Chaouki, J., Chehnoouni, A., Guy, C., Klvana, D. Preprints Eighth Engineering Foundation Conference Fluidization, Tours, Engineering Foundation. 1995: 681-688.

29. Hatano, H., Ishida, M. The entrainment of solid particles from a gas–solid fluidized bed. J. Chem. Eng. Jpn. 1981; 14:306-311.

30. Hartge, E.-U., Rensner, D., Werther, J. Solids concentration and velocity patterns in circulating fluidized beds. In: Basu, P., Large, J.F. Circulating Fluidized Bed Technology. Oxford: Pergamon Press. 1988(II):165-180.

31. Nakajima, M., Harada, M., Asai, M., Yamazaki, R., Jimbo, G. Bubble fraction and voidage in an emulsion phase in the transition to a turbulent fluidized bed. In Basu, P., Horio, M., Hasatani, M. Circulating Fluidized Bed III. Oxford: Pergamon Press. 1991:79-84.

32. Louge, M. Experimental techniques. In: Grace, J.R., Avidan, A.A., Knowlton, T.M. Circulating Fluidized Beds. London: Blackie Academic and Professional. 1997: 313-368.

33. Zhang, H, Johnston, P.M., Zhu, J.-X., de Lasa, H.I., Bergougnou, M.A. A novel calibration procedure for a fiber optic solids concentration probe. Powder Technology. 1998; 100:260-272.

34. Lirag, R.C., Litman, H. Statistical study of the pressure fluctuations in a fluidized bed. AIChE Symp. Ser. 1971; 166(67):11-22.

35. Brown, Robert C., Brue. Ethan Resolving dynamical features of fluidized beds from pressure fluctuations, Powder Technology. 2001; 119:68-80.

36. Kashkin, V.N., Lakhmostov, V.S., Zolotarskii, I.A., Noskov, A.S., Zhou, J.J. Studies on the onset velocity of turbulent fluidization for alpha-alumina particles. Chemical Engineering Journal. 2003; 91: 215-218.

37. Bi, H.T., Grace, J.R., Zhu, J. Propagation of pressure waves and forced oscillations in gas-solid fluidized beds and their influence on diagnostics of local hydrodynamics. Powder Technology. 1995b; 82:239-253.

38. Bi, H. T., Ellis, N., Abba, I. A., Grace, J. R. A state-of-the-art review of gas-solid turbulent fluidization, Chemical Engineering Science. 2000; 55:4789-4825.

39. Fan, L.T., Ho, Tho-ching, Hiraoka, S., Walawender, W.P. Pressure fluctuations in a fluidized bed. AIChE Journal. 1981; 27(3):388-396.

40. Du, Bing, Warsito, W., Fan, Liang-Shih Bed nonhomogeneity in turbulent gas-solids fluidization, AIChE Journal, 2003; 49(5):1109-1126.

41. Makkawi, Y. T., Wright, P. C. Fluidization regimes in a conventional fluidized bed characterized by means of electrical capacitance tomography. Chemical Engineering Science. 2002; 57:2411-2437.